Electronic Supplementary Material (ESI) for Inorganic Chemistry Frontiers.

Supporting Information

Efficient iodine capture by metal–organic cubes based on hexanuclear vanadium cluster

Yang Yang,[a] Yaomei Fu,[b] Yiran Tian,[a] Liang Zhao,*[a] Chao Qin, [a] Xinlong Wang*[a,c] and Zhongmin Su[a,c]

[a] *Key Laboratory of Polyoxometalate and Reticular Material Chemistry of Ministry of Education, Northeast Normal University, Changchun, 130024, China.*

[b] *Shandong Peninsula Engineering Research Center of Comprehensive Brine Utilization, Weifang University of Science and Technology, Shouguang, 262700, China.*

[c] *College of Science, Hainan University, Haikou 570228, China.*

Email: zhaol352@nenu.edu.cn; wangxl824@nenu.edu.cn

Experimental section

General Information

Commercial reagents in this work were used as received unless specially stated. The experiments were performed under an argon atmosphere using standard Schlenk techniques. ^{1}H NMR spectra were recorded at 25°C on a Bruker Avance 500 MHz NMR spectrometer and TMS as internal standard. The FT-IR spectra were performed in the range 3500–500 cm^{-1} using KBr pellets on an Alpha Centaurt FT/IR spectrophotometer. PXRD patterns were recorded from 5 to 50° at room temperature on a Siemens D5005 diffractometer with Cu *K*α (*λ* = 1.5418 Å). Thermogravimetric analysis (TGA) of the samples was performed using a Perkin Elmer TG−7 analyzer heated from 50 to 800°C under nitrogen at heating rate of 10°C min^{-1}. Elemental analyses (CHN) were conducted on a Perkin Elmer 2400 CHN elemental analyzer. The UV-Vis spectra were measured at room temperature using a VU-2550 UV-Vis Spectrophotometer. All data collections were performed on a Bruker D8–Venture diffractometer with a Turbo X-ray Source (Cu *K*α radiation, *λ* = 1.5418 Å) adopting the direct drive rotating anode technique and a CMOS detector at 173 K. The data frames were collected using the program APEX 3 and processed using the program SAINT routine in APEX 3. The structures were solved by direct methods and refined by the full1matrix least-squares on F^2 using the SHELXL–2014 program. CCDC 2278526 and 2278527 (**VMOC-6** and **VMOC-7**) contain supplementary crystallographic data for this paper.

Materials and methods

Synthesis of H_4PBPTA

P-cyanoacetophenone (80 mmol), 1,4-phthalaldehyde (20 mmol), and NaOH (80 mmol) were added to 200 mL of ethanol solution and stirred at room temperature for about 15 hours. Afterward, 80 mL of ammonia was added and stirred for another 24

h at room temperature. The solid was obtained by filtration, washed 3 times with ethanol, and dried in an oven. The solid was then transferred to aqueous 2 M NaOH (200 mL) and heated to reflux until there was no change in the color of the moist pH indicator paper. The reaction mass was cooled to room temperature and the solid in the reaction mass was filtered. The filtrate was acidified with dilute hydrochloric acid to pH = 1. The solid was precipitated, filtered and dried in an oven. Recrystallization in DMF and EtOH gave the product H_4PBPTA (4.0 g, about 29% yield). ^{1}H NMR (DMSO, 500 MHz). δ = 13.13 (s, 4H), 8.53 (d, 8H), 8.48 (s, 4H), 8.33 (s, 4H), 8.14 (d, 8H).

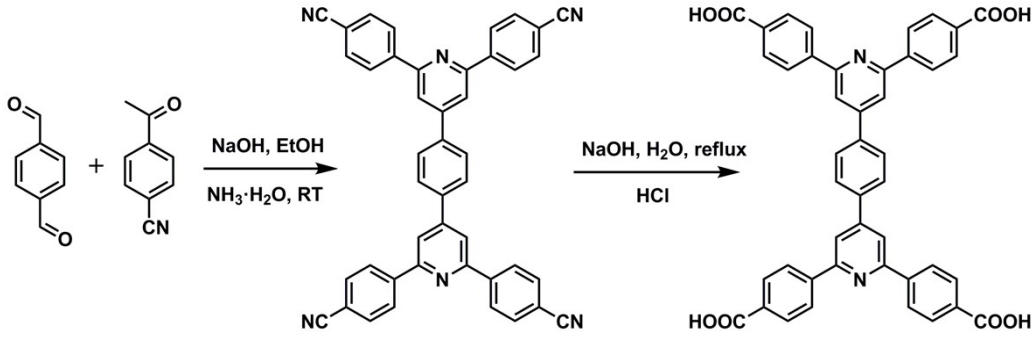

Scheme S1. Synthetic routes to H_4PBPTA.

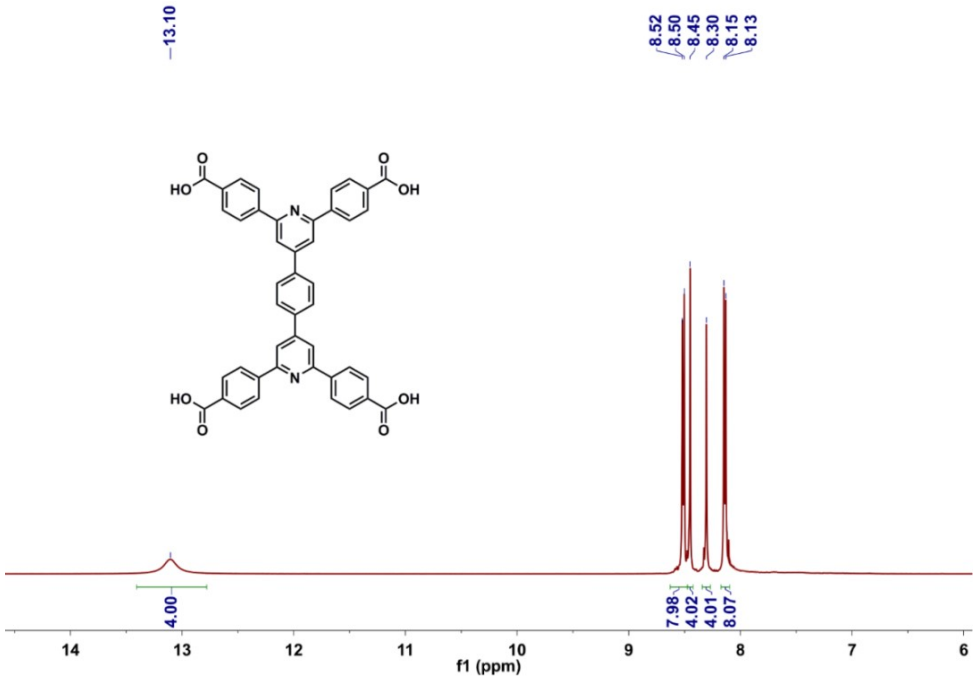

Fig. S1. ^{1}H NMR spectrum of H_4PBPTA in DMSO-d_6.

Table S1. The Crystallographic data for **VMOC-6** and **VMOC-7**.

Compound	**VMOC-6**	**VMOC-7**
Empirical formula	$C_{68}H_{488}N_{28}O_{200}S_8V_{48}$	$C_{384}H_{544}N_{36}O_{200}V_{56}$
Formula weight	11205.43	11717.16
Temperature/K	173.02	173.02
Crystal system	triclinic	triclinic
Space group	$P\bar{1}$	$P\bar{1}$
a/Å	29.845(5)	29.601(3)
b/Å	30.189(5)	29.920(3)
c/Å	31.613(5)	31.343(3)
α/°	86.200(7)	87.224(4)
β/°	71.393(6)	71.212(4)
γ/°	72.653(7)	73.450(4)
Volume/Å^3	25754(7)	25162(5)
Z	1	1
ρ_{calc}/g·cm^{-3}	0.723	0.733
μ/mm^{-1}	3.987	4.522
F(000)	5724.0	5988.0
Radiation	Cu *K*α (*λ* = 1.54178)	Cu *K*α (*λ* = 1.54178)
Theta range for data collection/°	4.176 to 62.18	3.814 to 62.386
Index ranges	-18 ≤ *h* ≤ 19, -19 ≤ *k* ≤ 20, -21 ≤ *l* ≤ 21	-19 ≤ *h* ≤ 19, -20 ≤ *k* ≤ 19, -20 ≤ *l* ≤ 20
Reflections collected	50315	63339
Independent reflections	15919 [R_{int} = 0.0897, R_{sigma} = 0.1056]	15774 [R_{int} = 0.1002, R_{sigma} = 0.1037]
Data/restraints/parameters	15919/8921/2502	15774/7541/2500
Goodness-of-fit on F^2	1.065	1.059
Final *R* indexes [$I \geq 2\sigma(I)$][a]	R_1 = 0.0823 wR_2 = 0.2229	R_1 = 0.1080 wR_2 = 0.2882
Final *R* indexes [all data][b]	R_1 = 0.1102 wR_2 = 0.2448	R_1 = 0.1498 wR_2 = 0.3244
Largest diff. peak/hole/eÅ^{-3}	0.55/-0.70	0.43/-0.51

$^{a}R_1=\sum||F_o|-|F_c||/\sum|F_o|$; $^{b}wR_2=\{\sum[w(F_o^2-F_c^2)^2]/\sum[w(F_o^2)^2]\}^{1/2}$

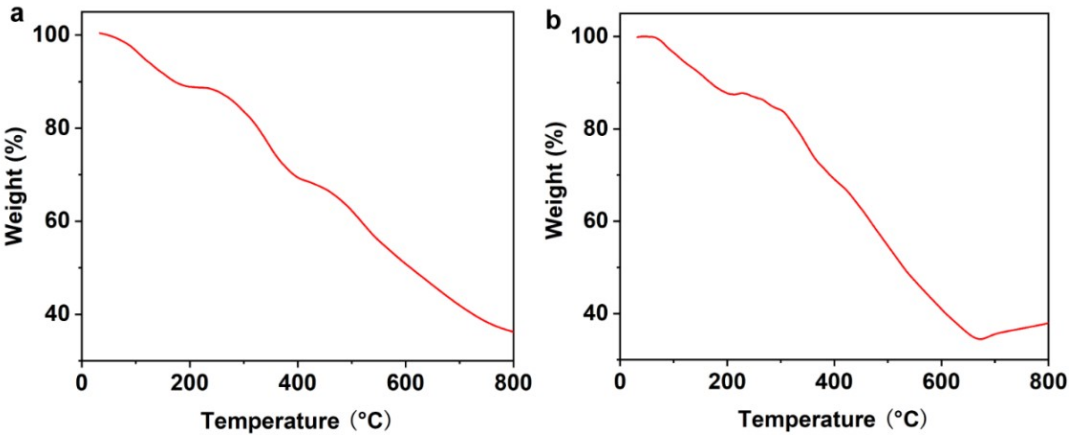

Fig. S2. TGA curves of **VMOC-6** (a) and **VMOC-7** (b).

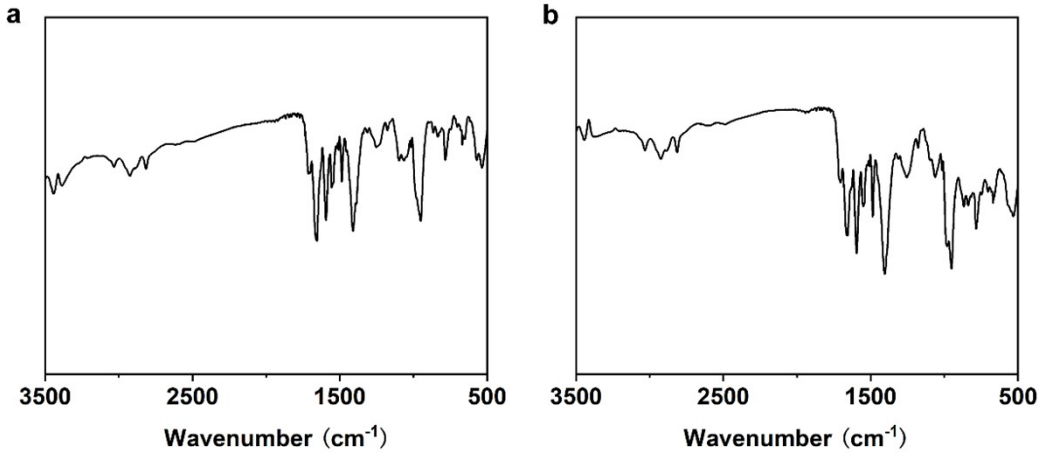

Fig. S3. The IR spectra of **VMOC-6** (a) and **VMOC-7** (b).

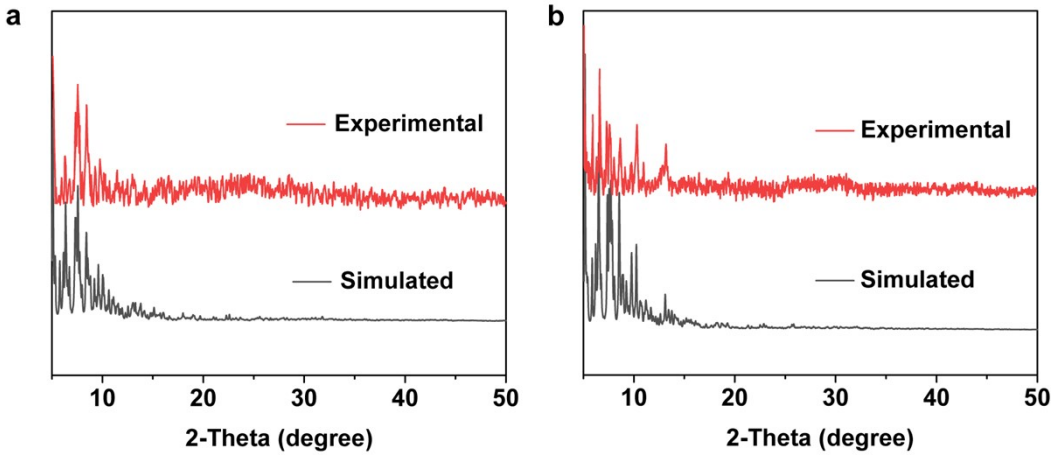

Fig. S4. The experimental and simulated PXRD patterns of **VMOC-6** (a) and **VMOC-7** (b).

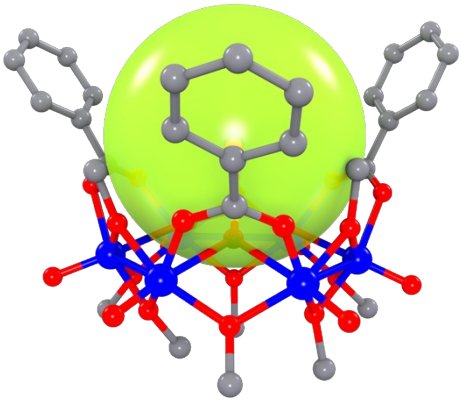

Fig. S5. Concave hexanuclear vanadium cluster structure.

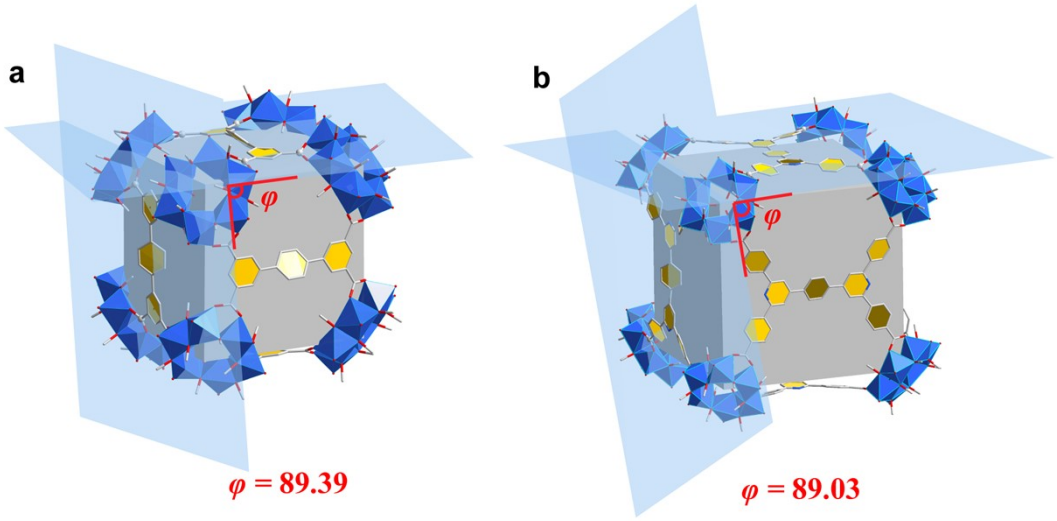

Fig. S6. The dihedral angles of **VMOC-4** and **VMOC-6**.

Table S2. The side and angle parameters of η and φ for **VMOC-4** and **VMOC-6**.

	***η*/°**	**η/°**	***φ* (dihedral angle/°)**	***φ*/°**	***a* (side/Å)**	***a*/Å**
VMOC–4	η_1 = 64.23	64.27	φ_1 = 89.64	89.39	a_1 = 21.55	21.57

	η_2 = 63.99		φ_2 = 89.79		α_2 = 21.56	
	η_3 = 64.60		φ_3 = 88.75		α_3 = 21.60	
	η_1 = 59.66		φ_1 = 88.30		α_1 = 28.47	
VMOC–6	η_2 = 59.65	59.54	φ_2 = 89.44	89.03	α_2 = 28.17	28.36
	η_3 = 59.31		φ_3 = 89.36		α_3 = 28.44	

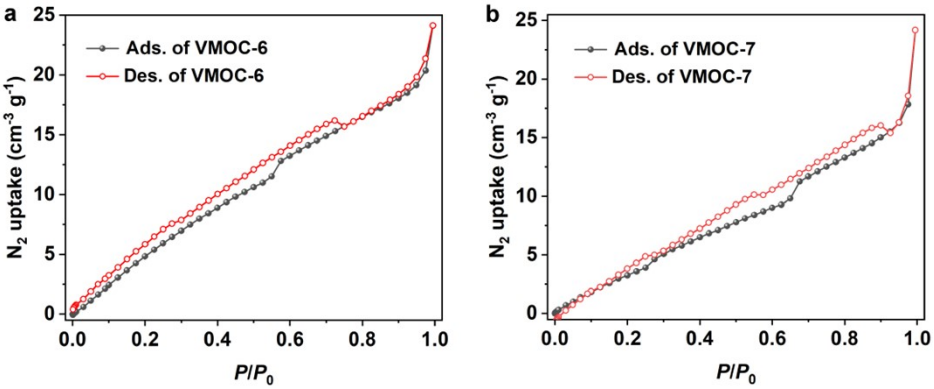

Fig. S7. N_2 adsorption-desorption isotherms of **VMOC-6** and **VMOC-7**.

Iodine Vapor Uptake

Iodine vapor uptake experiments were performed using the following procedure: the crystalline sample (20 mg) was weighed in a pre-weighed glass container (3 mL) and transferred to a larger sealed glass vial (20 mL) containing 800 mg of iodine at the bottom. There was no physical contact between the iodine and the caged sample as shown. The airtight container was then heated in an oven at 75°C. After iodine vapor adsorption, the cage with iodine was cooled to room temperature and weighed.

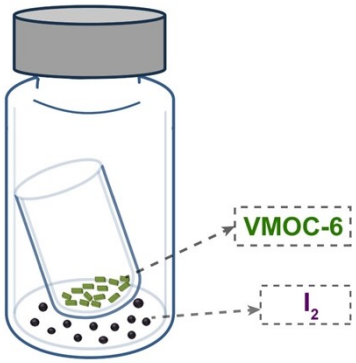

Fig. S8. Schematic diagram of iodine vapor uptake experiment.

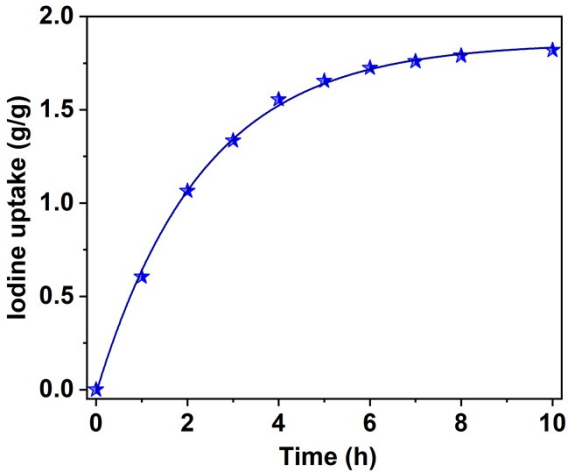

Fig. S9. Iodine vapor adsorption versus time for **VMOC-7** at 75°C and 1 atm.

Table S3. Comparison of iodine vapor adsorption in different metal–organic materials.

Metal–Organic Materials	category	Temperature (°C)	Time (h)	Iodine uptake ($g\ g^{-1}$)	Ref
IL@PCN-333(Al)	MOF	75	0.5–48	7.35	[1]
Cu@MIL-101	MOF	77	12	3.42	[2]
UPC-158-HF/HCl/HBr	MOF	70	20	2.19–2.92	[3]
UiO-66-FA	MOF	80	72	2.25	[4]
MOF-808	MOF	80	24	2.18	[5]
Zn_2(tptc)(apy)	MOF	75	60	2.16	[6]
VMOC-6	**MOP**	**75**	**10**	**1.83**	**This work**
UPC-158	MOF	70	20	1.78	[3]
HKUST-1	MOF	75	0.5–9	1.75	[7]
Cage-1	MOP	75	36	1.42	[8]
NU-1000	MOF	80	24	1.45	[5]
MFM-300(Sc/In/Fe/Al)	MOF	80	0.5–20	0.94–1.54	[9]
MFM-300(V^{III}/V^{IV})	MOF	70	48	1.25–1.42	[10]
ZIF-8	MOF	75	5–12	1.25	[11]
UiO-66	MOF	80	72	1.17	[4]
MBM	MOF	100	2	0.98	[12]

MOF-867	MOF	80	24	0.88	[5]
$[Cd(pbica)_2]\cdot 1.5DMF\cdot 2CH_3OH$	MOF	50	24	0.66	[13]
TMBP·CuI	MOF	77	0.5	0.64	[14]
Th-SINAP-13	MOF	80	6	0.60	[15]
UiO-67	MOF	80	24	0.53	[5]
HKUST-1@PES/PEI/PVDF	MOF	75	480	0.225–0.376	[16]
$[Zn_2(\mu_4\text{-}ao_2btc)(\mu\text{-}pbix)_2]$	MOF	75	3 d	0.20	[17]
$[Zn_3(BTC)_2(TIB)_2]$	MOF	70	4	0.04	[18]
$[Cd_3(BTC)_2(TIB)_2]$	MOF	70	4	0.03	[17]

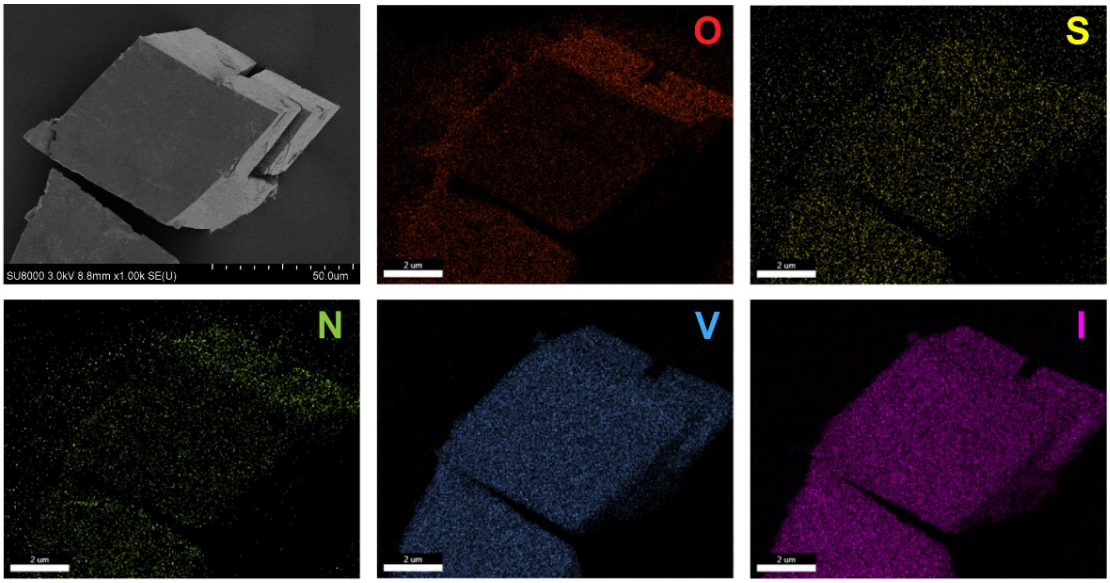

Fig. S10. Elemental mapping images of O, S, N, V and I for I_2-laden **VMOC-6**.

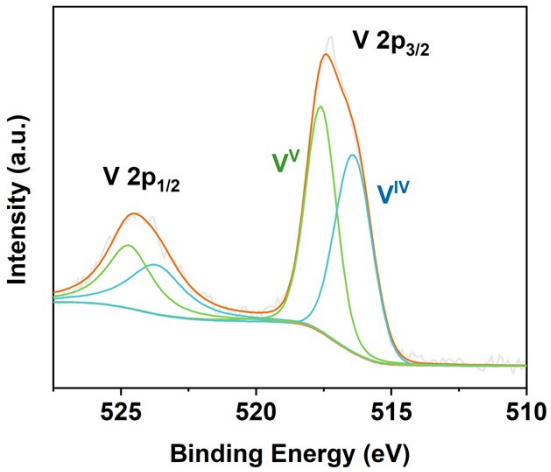

Fig. S11. XPS spectra of V 2p for I_2@**VMOC-6** derived signals.

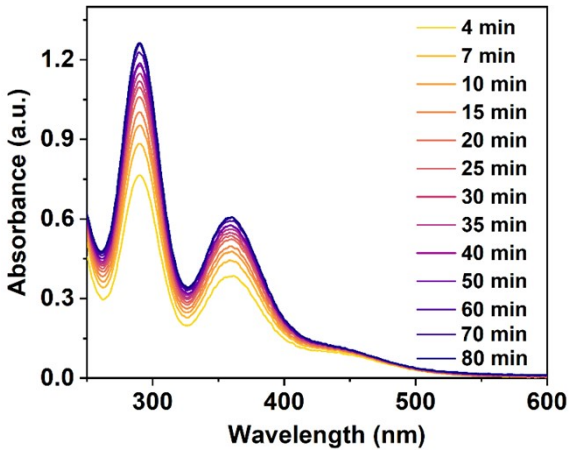

Fig. S12. Release of iodine from I_2@**VMOC–6** over 80 min.

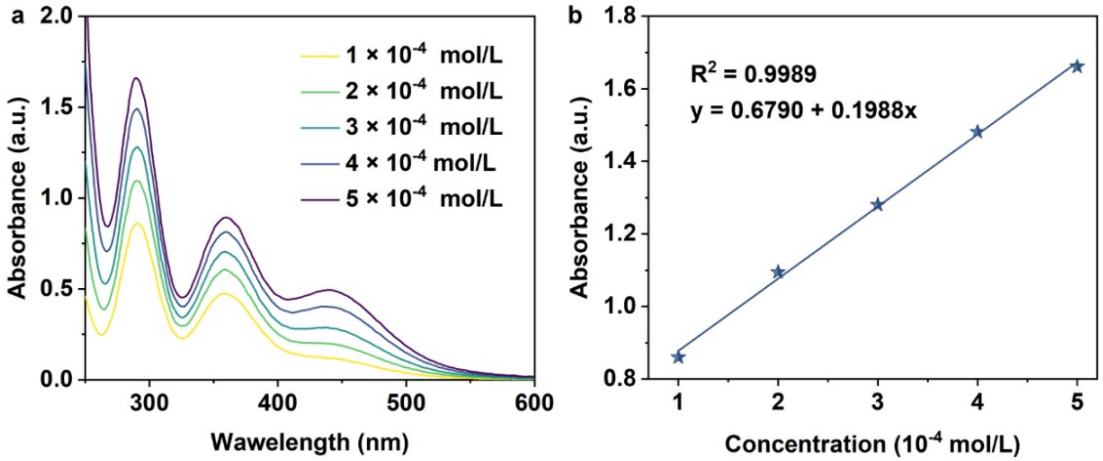

Fig. S13. (a) Calibration plot of standard iodine by UV-Vis spectra in MeOH solution. (b) The fitting of Abs value vs concentration of iodine in cyclohexane solution.

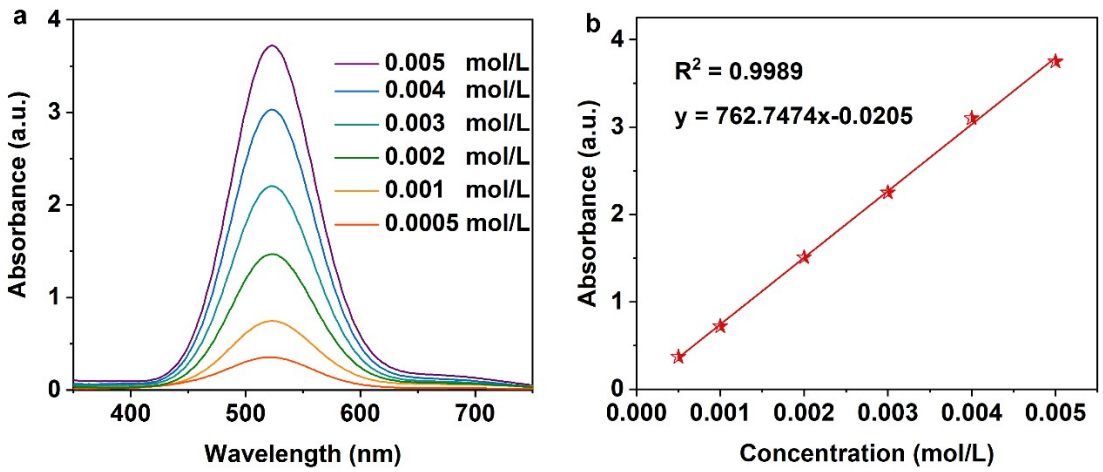

Fig. S14. (a) Calibration plot of standard iodine by UV-Vis spectra in cyclohexane solution. (b) The fitting of Abs value vs concentration of iodine in cyclohexane solution with the relatively good linearity satisfies Lambert-Beer Law.

References

1. Y. Tang, H. Huang, J. Li, W. Xue and C. Zhong, IL-induced formation of dynamic complex iodide anions in IL@MOF composites for efficient iodine capture, *J. Mater. Chem. A*, 2019, **7**, 18324–18329.
2. B. Qi, Y. Liu, T. Zheng, Q. Gao, X. Yan, Y. Jiao and Y. Yang, Highly efficient capture of iodine by Cu/MIL-101, *J. Solid State Chem.*, 2018, **258**, 49–55.
3. B. Guo, F. Li, C. Wang, L. Zhang and D. Sun, A rare (3,12)-connected zirconium metal–organic framework with efficient iodine adsorption capacity and pH sensing, *J. Mater. Chem. A*, 2019, **7**, 13173–13179.
4. J. Maddock, X. Kang, L. Liu, B. Han, S. Yang and M. Schröder, The Impact of Structural Defects on Iodine Adsorption in UiO-66, *Chemistry (Switzerland)*, 2021, **3**, 525–531.
5. P. Chen, X. He, M. Pang, X. Dong, S. Zhao and W. Zhang, Iodine Capture Using Zr-Based Metal-Organic Frameworks (Zr-MOFs): Adsorption Performance and Mechanism, *Acs Appl. Mater. Inter.*, 2020, **12**, 20429-20439.
6. R.-X. Yao, X. Cui, X.-X. Jia, F.-Q. Zhang and X.-M. Zhang, A Luminescent Zinc(II) Metal-Organic Framework (MOF) with Conjugated π-Electron Ligand for High Iodine Capture and Nitro-Explosive Detection, *Inorg. Chem.*, 2016, **55**, 9270–9275.
7. D. F. Sava, K. W. Chapman, M. A. Rodriguez, J. A. Greathouse, P. S. Crozier, H. Zhao, P. J. Chupas and T. M. Nenoff, Competitive I_2 Sorption by Cu-BTC from Humid Gas Streams, *Chem. Mater.*, 2013, **25**, 2591–2596.

8. W.-Y. Pei, J. Yang, H. Wu, W. Zhou, Y.-W. Yang and J.-F. Ma, A calix 4 resorcinarene-based giant coordination cage: controlled assembly and iodine uptake, *Chem. Commun.*, 2020, **56**, 2491–2494.
9. X. Zhang, I. da Silva, H. G. W. Godfrey, S. K. Callear, S. A. Sapchenko, Y. Cheng, I. Vitorica-Yrezabal, M. D. Frogley, G. Cinque, C. C. Tang, C. Giacobbe, C. Dejoie, S. Rudic, A. J. Ramirez-Cuesta, M. A. Denecke, S. Yang and M. Schroder, Confinement of Iodine Molecules into Triple-Helical Chains within Robust Metal–Organic Frameworks, *J. Am. Chem. Soc*, 2017, **139**, 16289–16296.
10. X. Zhang, I. da Silva, R. Fazzi, A. M. Sheveleva, X. Han, B. F. Spencer, S. A. Sapchenko, F. Tuna, E. J. L. McInnes, M. Li, S. Yang and M. Schroder, Iodine Adsorption in a Redox-Active Metal–Organic Framework: Electrical Conductivity Induced by Host-Guest Charge-Transfer, *Inorg. Chem.*, 2019, **58**, 14145–14150.
11. D. F. Sava, M. A. Rodriguez, K. W. Chapman, P. J. Chupas, J. A. Greathouse, P. S. Crozier and T. M. Nenoff, Capture of Volatile Iodine, a Gaseous Fission Product, by Zeolitic Imidazolate Framework-8, *J. Am. Chem. Soc*, 2011, **133**, 12398–12401.
12. T. He, X. Xu, B. Ni, H. Lin, C. Li, W. Hu and X. Wang, Metal–Organic Framework Based Microcapsules, *Angew. Chem. Int. Ed.*, 2018, **57**, 10148–10152.
13. B.-B. Shi, R.-Z. Pei, A.-W. Chen, C. Wang, Y.-M. Ma and Z. Yin, A rigid and porous metal-organic frameworks with 1D rhombus channels and double walls: Selective adsorption of CO_2 over N_2, iodine capture, and fluorescence, *Inorganic Chemistry Communications*, 2019, **102**, 147–151.
14. J. He, J. Duan, H. Shi, J. Huang, J. Huang, L. Yu, M. Zeller, A. D. Hunter and Z. Xu, Immobilization of Volatile and Corrosive Iodine Monochloride (ICl) and I-2 Reagents in a Stable Metal–Organic Framework, *Inorg. Chem.*, 2014, **53**, 6837–6843.
15. Z.-J. Li, Y. Ju, B. Yu, X. Wu, H. Lu, Y. Li, J. Zhou, X. Guo, Z.-H. Zhang, J. Lin, J.-Q. Wang and S. Wang, Modulated synthesis and isoreticular expansion of Th-MOFs with record high pore volume and surface area for iodine adsorption, *Chem. Commun.*, 2020, **56**, 6715–6718.
16. B. Valizadeh, T. N. Nguyen, B. Smit and K. C. Stylianou, Porous Metal–Organic Framework@Polymer Beads for Iodine Capture and Recovery Using a Gas-Sparged Column, *Adv. Funct. Mater.*, 2018, **28**, 1801596.
17. M. Arici, O. Z. Yesilel, M. Tas and H. Demiral, Effect of Solvent Molecule in Pore for Flexible Porous Coordination Polymer upon Gas Adsorption and Iodine Encapsulation, *Inorg. Chem.*, 2015, **54**, 11283–11291.
18. Y. Rachuri, K. K. Bisht, B. Parmar and E. Suresh, Luminescent MOFs comprising mixed tritopic linkers and Cd^{II}/Zn^{II} nodes for selective detection of organic nitro compounds and iodine capture, *J. Solid State Chem.*, 2015, **223**, 23–31.